Available on CMS information server

CMS NOTE 1998/043

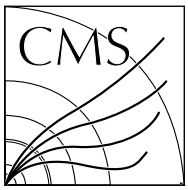

The Compact Muon Solenoid Experiment

CMS Note

Mailing address: CMS CERN, CH-1211 GENEVA 23, Switzerland

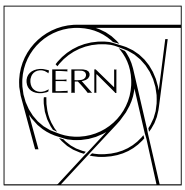

June, 1998

A method for the static characterisation of the CMS Tracker analogue optical links

G.Cervelli, V.Arbet-Engels, K.Gill, R.Grabit, C.Mommaert, G.Stefanini, F.Vasey
CERN, Geneva, Switzerland

Abstract

Analogue optical links are being developed for the CMS Tracker. The large number of optical channels (over 50,000) requires semi-automated test procedures and efficient evaluation criteria to compare different link solutions and to optimise their performance, whilst complying with system specifications. In addition, self-triggered calibration schemes need to be developed to maintain the readout chain accuracy during the detector lifetime (10 years).

In this paper we present a method for the static characterisation of the CMS analogue optical links, relying on an automated set-up for gain, rms-noise and linearity measurements, and on a software program for off-line processing of the test data. We propose a set of evaluation criteria and describe a compact representation of the results in the operational parameter space (dc working point, operating range). This representation allows quantification and comparison of the performance of links based on different components, as well as allowing development and simulation of practical testing and calibration procedures.

1. Introduction

A 50,000 fibre, 100 m long, optical link is being developed to read out analogue data from the $12 \cdot 10^6$ microstrip detector channels of the CMS tracker [1]. Data will be time multiplexed at a 256:1 ratio and transmitted at a rate of 40 MSamples/s (MS/s) [2]. The optical system architecture (shown in Fig. 1) will make use of directly modulated InGaAsP edge-emitting lasers (λ = 1310 nm), InGaAs pin-photodiodes, single mode fibres, and connectors [3, 4].

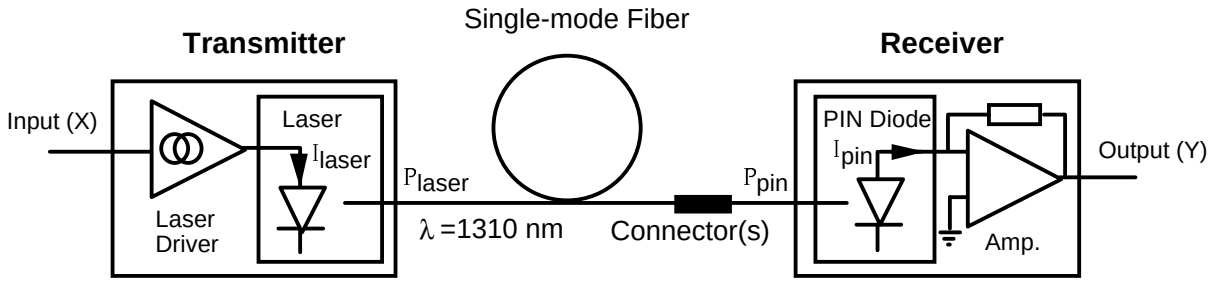

Figure 1: Schematic of the optical link prototype, with the laser transmitter (left) and the pin-diode photoreceiver (right).

When operating the optical link, a certain number of free parameters (such as the dc working point of the laser and the width of the operating range) need to be chosen and adjusted by the user in order to optimise the performance of the read-out system. This choice requires the capability to quantitatively assess the link performance as function of the operating parameters.

In this paper we present a method for the static performance evaluation of the optical link and we describe a partially automated set-up for its characterisation. We define two static evaluation criteria: deviation from linearity and signal to noise ratio. Based on a single measurement of the link characteristic functions, its operation is simulated off-line for variable working points and its static performance is evaluated in a multi-dimensional parameter space. Given this compact representation of the results, the operating range of the link can then be mapped onto a region where a good compromise between linearity deviation and signal to noise ratio exists.

Once an operating point and a working range have been identified, the system must be calibrated on-line and the calibration parameters must be extracted and passed on to the signal processing electronics. The definition of an appropriate static evaluation method allows development, simulation and comparison of practical testing and calibration procedures. It is a major step towards the implementation of an optimised analogue optical link for the CMS Tracker.

In Section 2, we introduce the basic concepts of system operation, necessary to understand the sources of error in the analogue data transmission across the system. We then describe, in Section 3, the automated set-up for static performance characterisation. Section 4 defines the two static evaluation criteria (deviation from linearity and signal to noise ratio) and presents the compact representation of the performance in the parameter space. The off-line evaluation procedure is described in Section 5 and demonstrated with real data. A short discussion on practical re-calibration schemes follows in Section 6.

2. System operation and calibration

The analogue link response (output as a function of input) can be written in the form [6]:

$$Y = f(X) + n(X,t) \tag{1}$$

where X is the input signal, $f(X)$ is a deterministic function describing the average static characteristic response of the system (static transfer function), and $n(X,t)$ is a centred noise whose stochastic properties may depend on X (noise function).

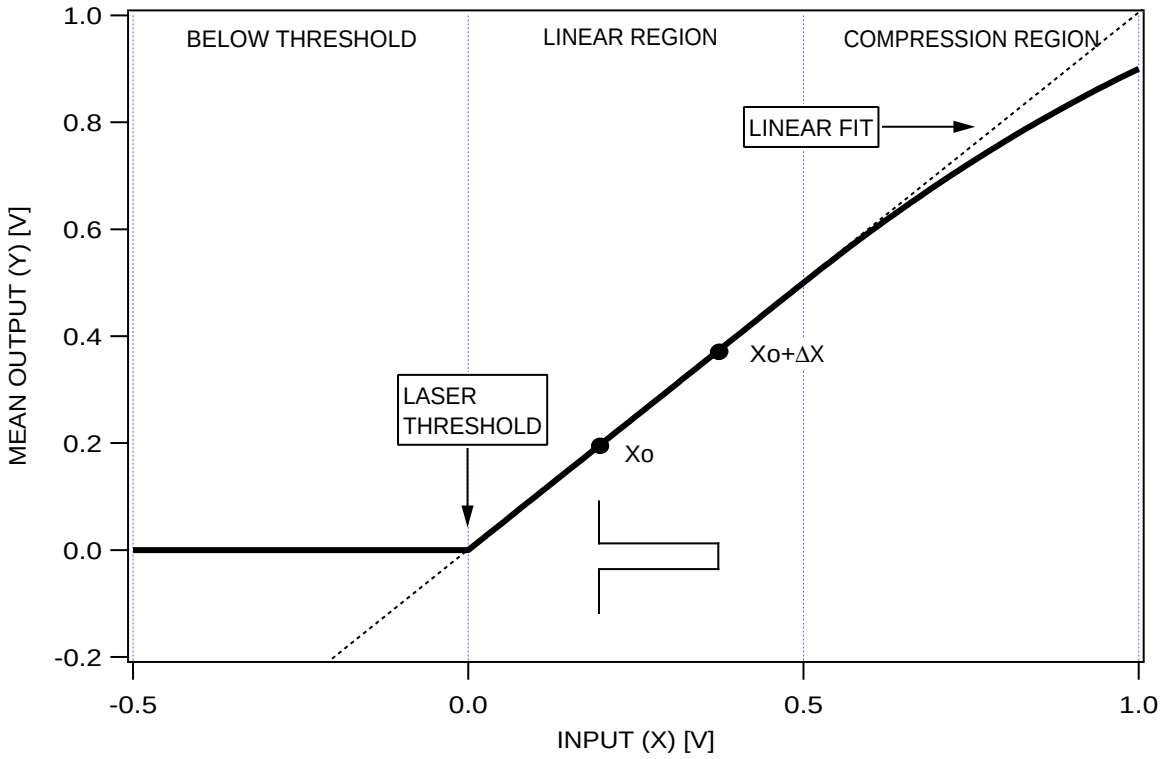

(a)

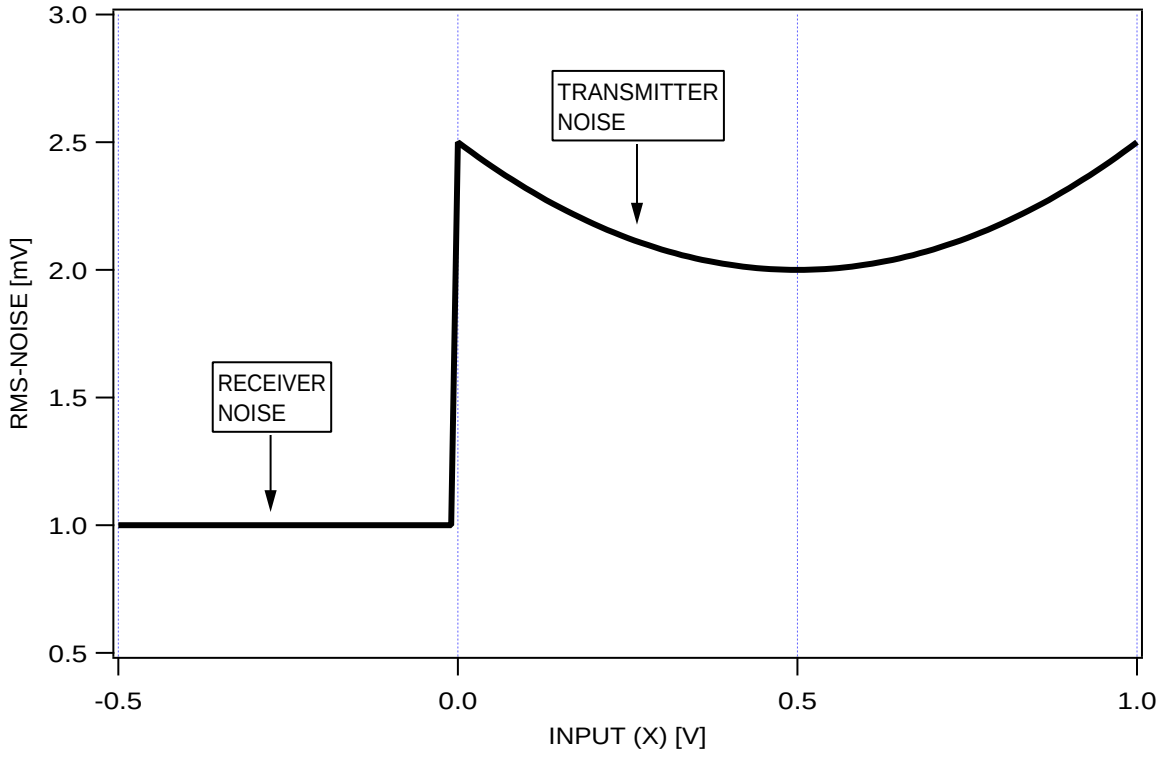

(b)

Figure 2: Idealised laser link characteristic functions: (a) output voltage and (b) rms-noise as a function of the input voltage. These synthesised functions are used to demonstrate the concepts and methods used for static evaluation.

As an example, Fig. 2 shows synthesised functions representative of laser link behaviour (the use of idealised functions is convenient to introduce operation and evaluation concepts; in Section 4, the same concepts will be demonstrated on real data). Fig. 2a shows a static transfer function $f(X)$. The input X is the drive voltage of the laser driver, and the output Y is the voltage at the output of the photoreceiver. The output voltage is proportional to the light collected by the photoreceiver. The abrupt nonlinearity at X=0 reflects the presence of a laser threshold. Below threshold (X<0), there is no coupling between the input and the output, and the noise seen is the photoreceiver noise. Above threshold a laser optical power is generated and is coupled into the fibre. The slope of the static transfer function in this region is proportional to the laser slope efficiency. To analyse the effect of a smooth nonlinearity, the link function is made nonlinear in the region X > 500 mV. This is a typical compression function, which can be observed in the laser itself or can be due to saturation effects in the amplifiers. Fig. 2b shows the root-mean-square (rms) of a noise function $n(X,t)$, or rms-noise function. While the only noise contribution below threshold (X<0) is due to the receiver, the transmitter noise dominates above threshold. It has a peak close to threshold, goes through a minimum, and then increases again as a function of the emitted optical power.

In an ideal link, the response $f(X)$ would be a linear function of the input X and the noise component $n(X,t)$ should be negligible with respect to $f(X)$, so that $Y \sim f(X)$, and the value of X could be determined precisely from the measurement of Y. However, in practice, these conditions are satisfied within a certain approximation and for a given range of input values. The linear estimation X_{est} of X, based only on the measurement of Y, relies on the approximation with a regression line of the static transfer function:

$$Y \approx f(X_0) + G \cdot (X - X_0) \tag{2}$$

where X_o is the working point, and G is the slope of the regression line around X_o. We define X_o and G as the optical link calibration parameters. The equation used to infer the input signal X from the output Y is:

$$X_{est} = \frac{Y - f(X_0)}{G} + X_0 \approx X \tag{3}$$

Clearly, the static performance (accuracy of X_{est}) of a given system depends on the choice of the calibration parameters, X_o and G, and on the absolute value of X within the operating range.

The working point X_o defines the analogue link baseline during operation, and the information to be transmitted is coded as the input swing X-X_o (Pulse Amplitude Modulation). Ideally, X_o has to be chosen so that the input range fits into a portion of the characteristic showing good linearity and high signal to noise ratio (SNR).

For a given X_o, the portion of the characteristic corresponding to the input range can be fitted with a straight line, and the parameter G can be calculated. As an example, the simplest way to define G is by drawing a regression line between two points on the static characteristic, as shown in Fig. 2. The first point is the working point (X_o, $f(X_o)$), and the second is the calibration point ($X_o+\Delta X$, $f(X_o+\Delta X)$), generated by applying a calibration pulse ΔX (positive or negative) at the system input. Thus the regression slope G is given by:

$$G \equiv \frac{f(X_0 - \Delta X) - f(X_0)}{\Delta X} \tag{4}$$

The calibration pulse is a reference input, injected into the link, whose amplitude ΔX must be known with good precision.

This fitting procedure for the determination of the parameter G is well adapted to our application. It is easy to implement in a practical system, and appears to give good results from the point of view of the static performance characterisation (as shown in Sections 4 and 5).

3. Experimental Set-up and measurements

The purpose of the characterisation of the system is to evaluate its static transfer function $f(X)$ and the stochastic properties of its noise function $n(X,t)$, as a function of the input voltage X. To do so, repeated measurements of Y (output) must be taken for a stable X (input). For each level X, the statistic of the output is evaluated, giving as a result the static transfer function $f(X)$ (systematic component) and the rms-noise function (standard deviation).

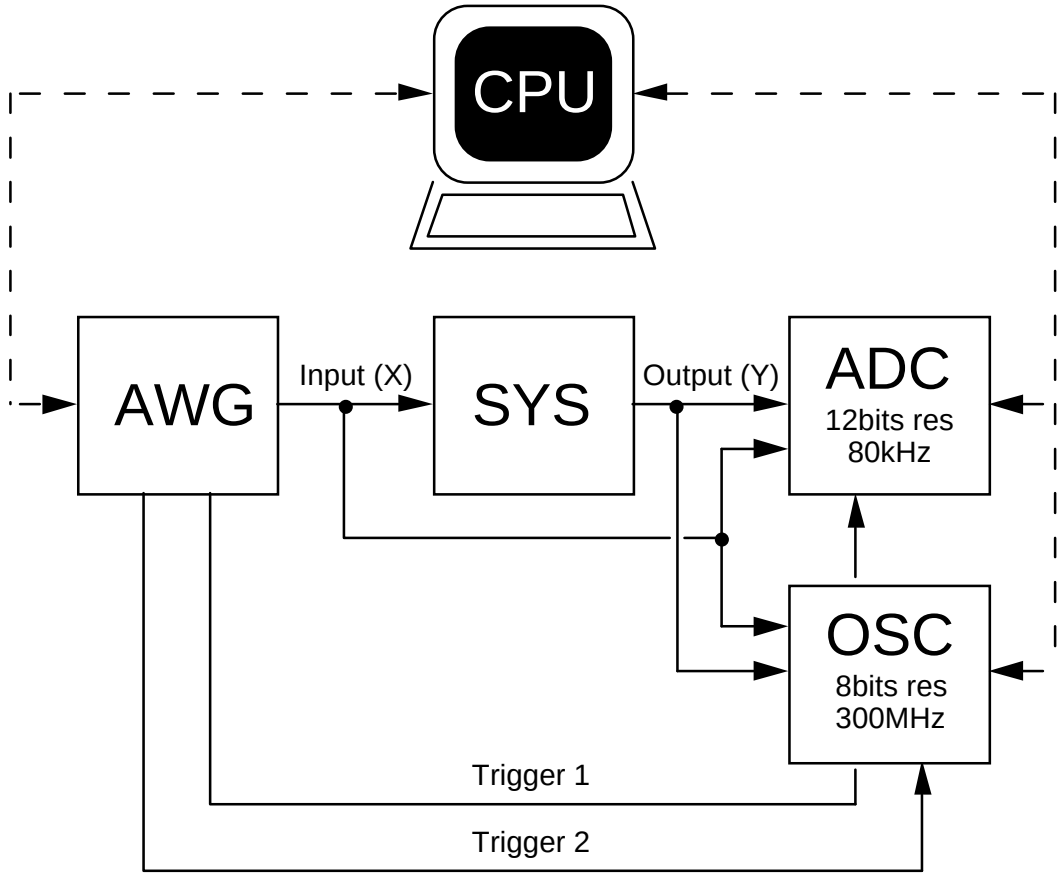

Figure 3: Automated set-up used for the static measurements. The Arbitrary Waveform Generator (AWG) provides programmable dc input levels to stimulate the system. The ADC and oscilloscope sample the system output at discrete times triggered by the AWG. The three instruments are controlled by a central processor running LabVIEW software.

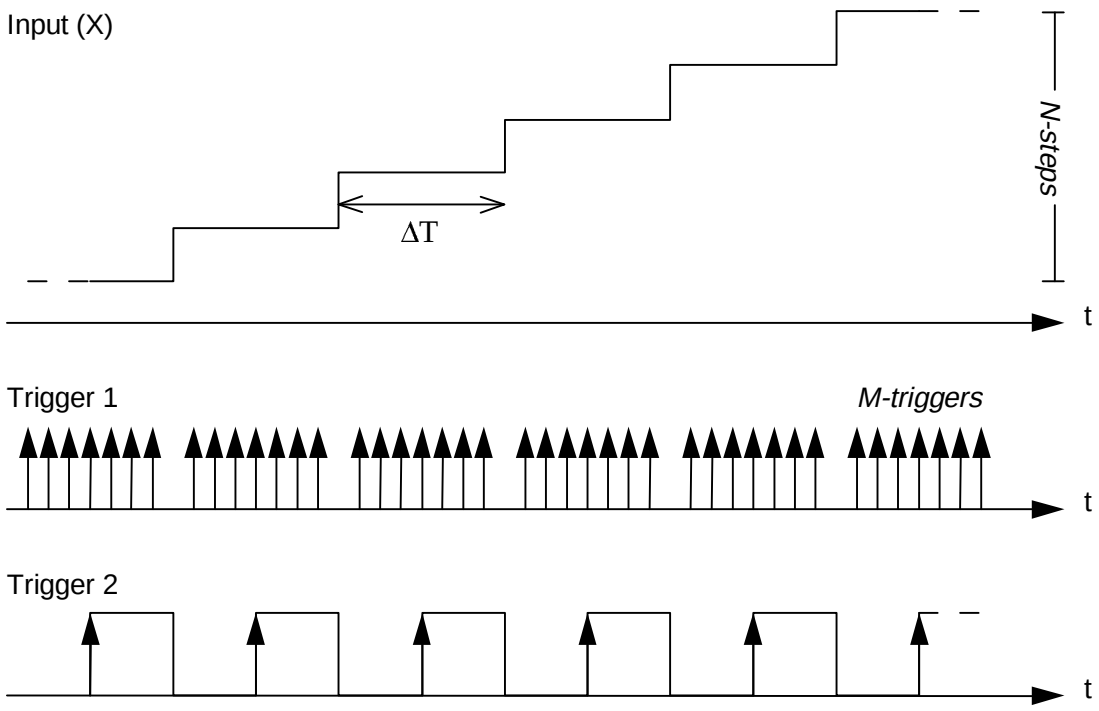

Figure 4: Input grid and synchronisation data as generated by the Arbitrary Waveform Generator (AWG).

The set-up described in this section, schematically shown in Fig. 3, is quite general and can be used to characterise any system with voltage inputs and outputs. The arbitrary waveform generator (AWG) generates input dc levels and synchronisation signals; one or more instruments monitor the system output; the controller communicates and exchanges data with the instruments on a parallel bus. The input levels are generated in steps covering the input range of interest with the programmed resolution (Fig. 4). Each level X is held for a time DT allowing repeated acquisitions of the output Y, as triggered by the generator (trigger 1). All the measurements are controlled by a central processor running LabVIEW software.

The basic requirements for the instrumentation are as follows. (a) A high measurement resolution is needed for the evaluation of $f(X)$, and subsequent evaluation of linearity to better than a few 1/1000 (>10bits). (b) A high measurement bandwidth (>200MHz) is needed to give an accurate estimation of the system noise. (c) The input must be stable not to introduce significant noise on the output. (d) The full acquisition must take less than a few seconds (to minimise time instabilities in the system).

A good compromise is obtained by using two separate instruments to monitor the output. A 12 bits low analogue bandwidth ADC board is used as a stand-alone VME module to sample the DC-coupled output and give good estimations of $f(X)$, after averaging over repeated acquisitions (requirement a). The rms-voltmeter function of a 300 MHz digital scope is used to measure the AC-coupled noise power, averaged over 5000 points (requirement b). A full acquisition of $f(X)$ for ~100 points takes less than a second (requirement d).

Figure 5 shows the static transfer function and the rms-noise function of a laser link prototype [7]. The linear region of the static transfer function is limited by the laser threshold (bottom) and by the receiving amplifier saturation at 3.5V (top). The devices gains are still being optimised, and the overall gain might not be representative of the final system values.

4. Evaluation criteria

Given the system representation of eq. 1 and the definition of X_{est} (eq. 3), the estimation errors have both a systematic component, due to the nonlinear transfer function $f(X)$, and a stochastic component, due to the noise function $n(X,t)$.

The estimation errors are therefore stochastic functions, and the evaluation criteria described in this section quantify their properties (mean and rms-value) as a function of the calibration parameters (X_o, G). Based on the evaluation results, optimisation procedures then guide the choice of the calibration parameters, so as to yield an acceptable error over the operating range (as described in the following Section).

The absolute and relative estimation errors are:

$$\begin{aligned} \varepsilon_a(X,t) &\equiv X_{est} - X \\ \varepsilon_r(X,t) &\equiv \frac{\varepsilon_a(X,t)}{X - X_0} \end{aligned} \tag{5}$$

4.1 Linearity Error

The deviation from linearity (or linearity error) is defined as the mean of the estimation error. This is given in absolute and relative terms by the following equations:

$$\begin{aligned} \varepsilon_{al}(X) &\equiv \overline{X}_{est} - X = \frac{f(X) - f(X_0)}{G} + X_0 - X \\ \varepsilon_{rl}(X) &\equiv \frac{\varepsilon_{al}(X)}{X - X_0} = \frac{f(X) - f(X_0) - G \cdot (X - X_0)}{G \cdot (X - X_0)} \end{aligned} \tag{6}$$

The linearity error depends on the choice of the working point X_o and of the calibration pulse amplitude ΔX (through G). As an example, Fig. 6 shows the relative linearity error corresponding to the transfer function of Fig. 2a and to different choices of X_o (for ΔX = 200 mV). By definition, the absolute linearity error is null at the two calibration points X_o and $X_o+\Delta X$. The normalisation by X-X_o leads to an undefined relative linearity error in X_o. A good choice of the calibration points leads to a rather flat relative linearity error around $X_o+\Delta X$, where the link should be operated. The operating input range can be, for instance, the interval [X_o, $X_o+k\cdot\Delta X$], where the value of k (k>1) is dictated by a trade-off between linearity and dynamic range.

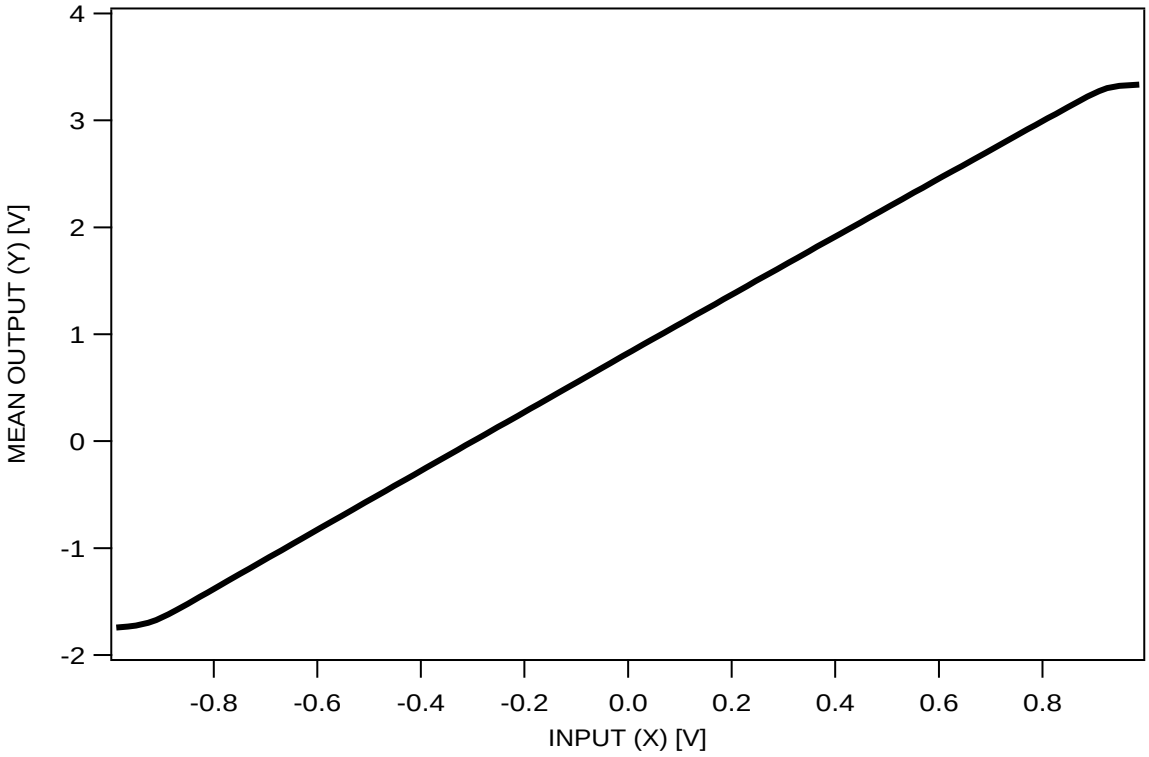

(a)

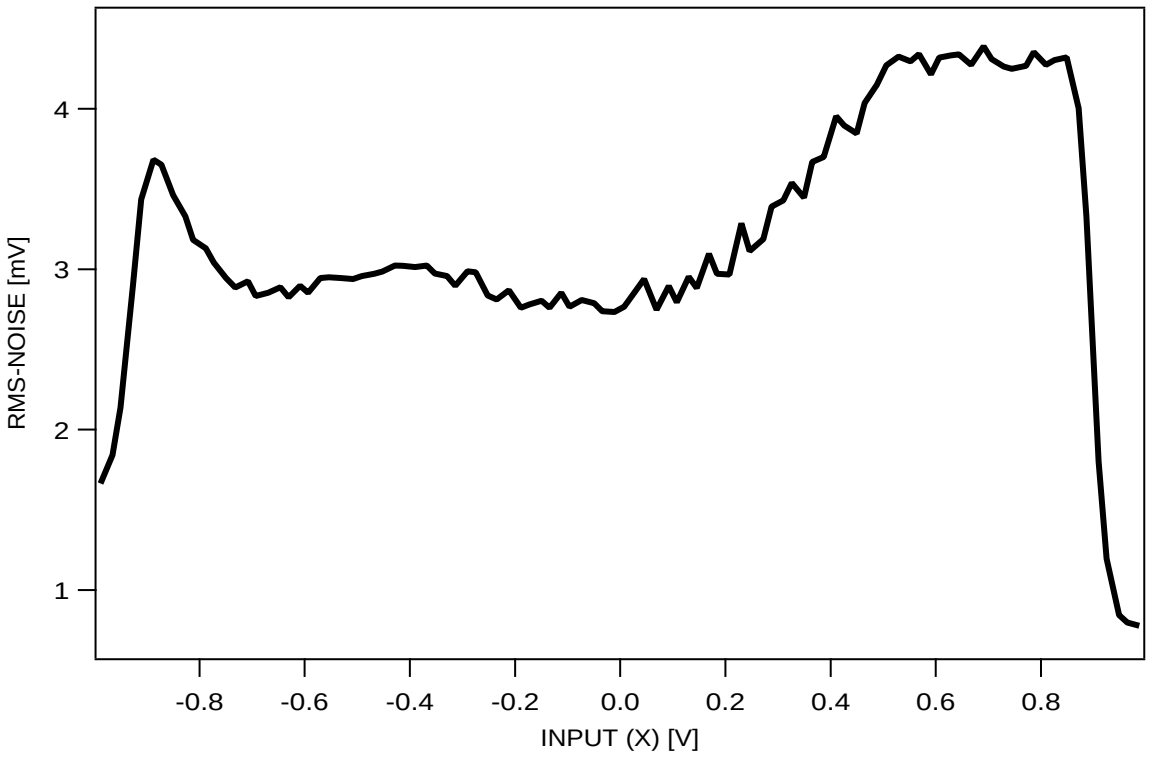

(b)

Figure 5: Transfer and noise characteristics of a real optical link prototype (NEC laser, pin-photodiode, and FC/PC connector).

In Fig. 7, the relative linearity error is represented in grey levels as a function of the input signal X and of the working point X_o (for ΔX = 200mV). The projections at X_o = 100, 250, 350, and 400 mV, shown in Fig. 6, are also indicated as a reference in Fig. 7.

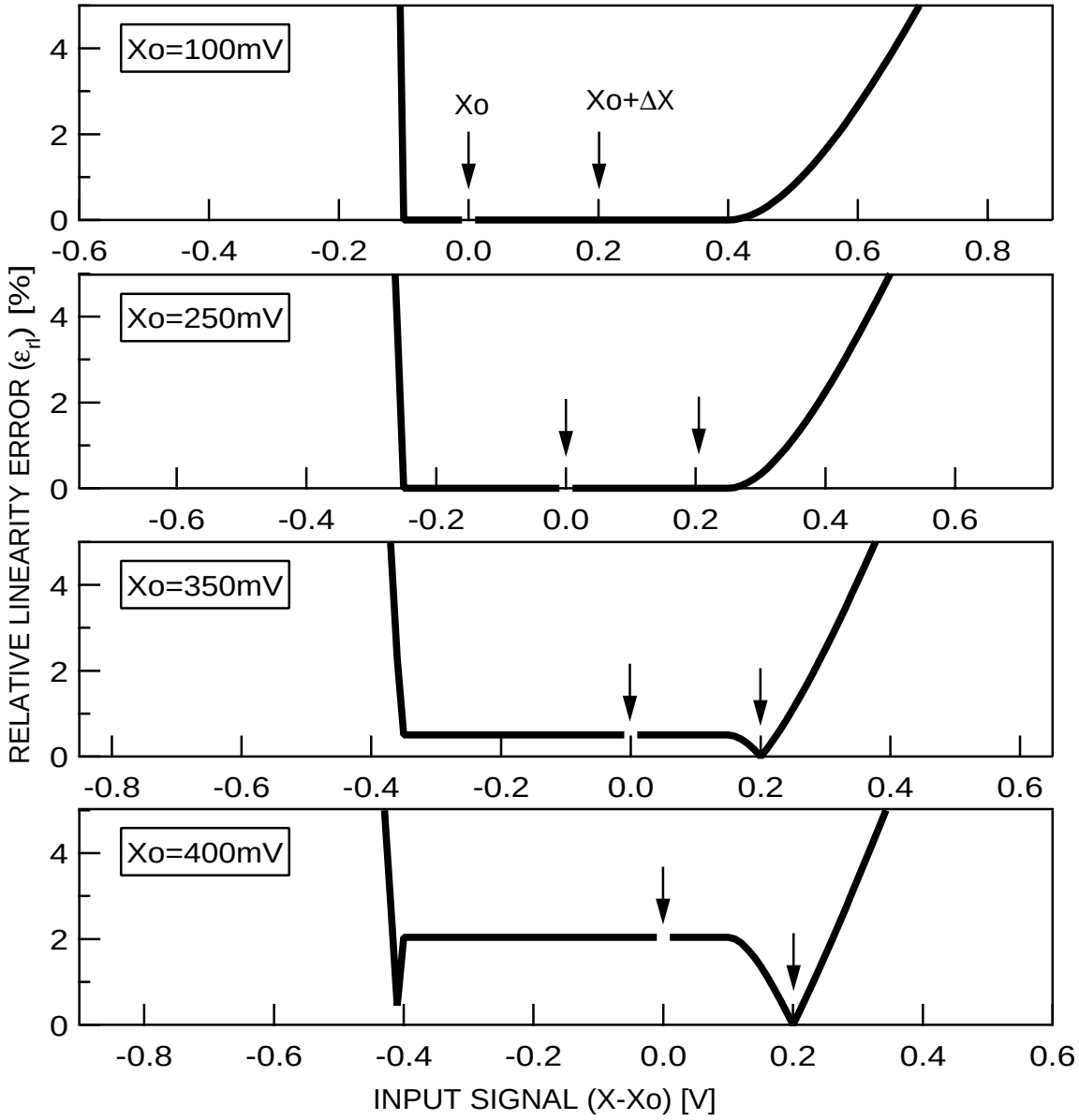

Figure 6: Relative linearity error as a function of X, for parameterised values of X_o (ΔX = 200 mV). The system is the one modelled by the functions represented in Fig. 2. Arrows indicate the two points X_o and $X_o+\Delta X$.

4.2 Signal to Noise Ratio

The standard deviation of the estimation error is the rms-noise function itself. This needs to be compared to the signal, in order to give an evaluation of the dynamic range of the system. We therefore introduce the signal-to-noise ratio (SNR) as:

$$\mathrm{SNR}(X) \equiv \frac{|f(X) - f(X_0)|}{\sqrt{n^2(X,t)}} \tag{7}$$

The SNR depends on the working point X_o. Figure 8 shows the SNR corresponding to the transfer and rms-noise functions of Fig. 2 and to different choices of X_o. By definition (eq. 7), the SNR is null for X=X_o. As X-X_o

increases, the SNR increases accordingly. If the rms-noise were constant, the SNR would increase linearly with X-X_o. The observed saturation is due to the noise increase and compression of the transfer function.

In the region where $X<0$ (under threshold), $f(X)$ is constant. Thus the difference $|f(X) - f(X_o)|$ is also constant, for a given X_o, and the SNR saturates to a constant value. This value is eventually better than the one obtained above threshold ($X>0$), since a lower noise has been assumed for $X<0$ (see Fig. 2). However, this region of the operating range cannot be exploited for analogue transmission, because of the bad linearity figure (see Fig. 7).

In Fig. 9 a contour plot of the SNR is represented as a function of the input signal X and of the working point X_o.

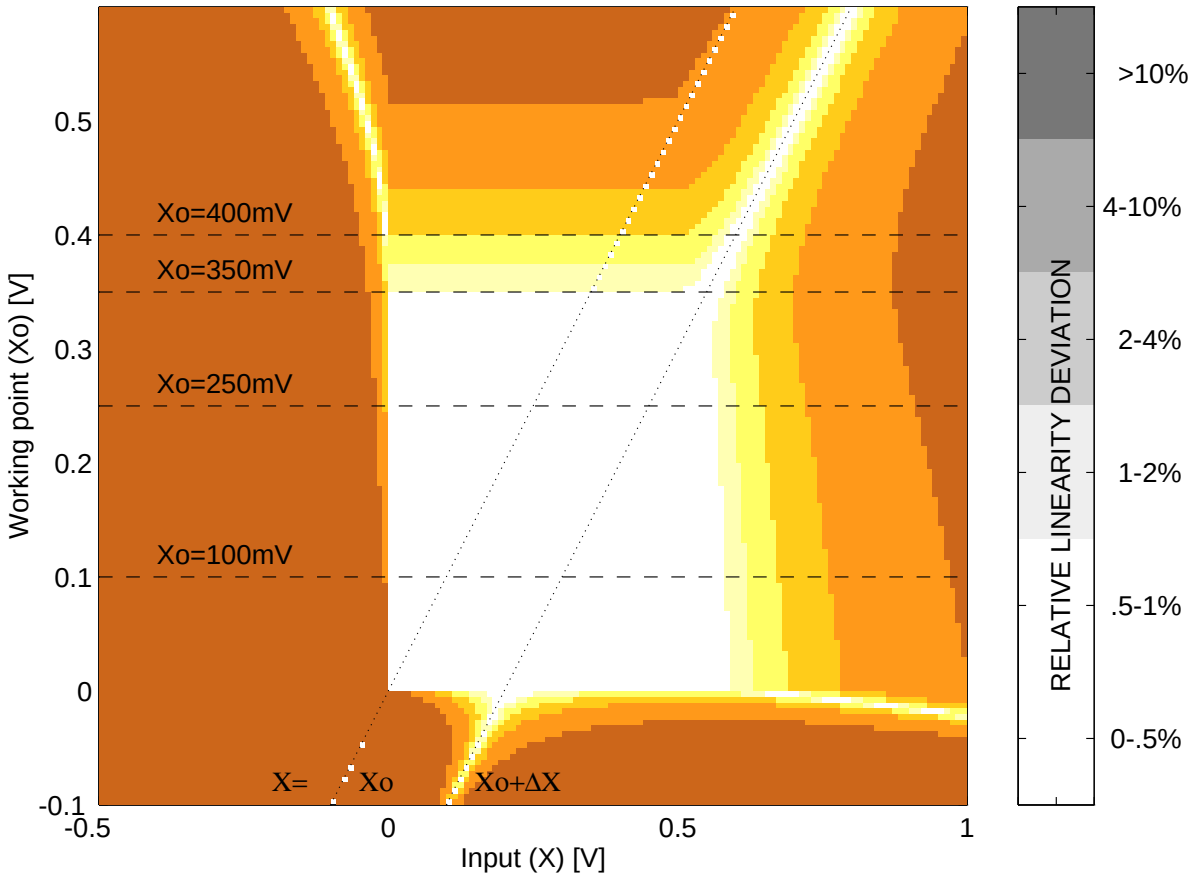

Figure 7: Pseudo-colour representation of the relative linearity error in the (X, X_o) space (ΔX = 200 mV). The system is the one modelled by the functions represented in Fig. 2.

4.3 Compact Representation of the Static Performance

As can be seen by comparing Fig. 7 and 9, linearity error and SNR measurements can thus be superimposed on a same plot (such as the one in Fig. 10) containing all the necessary information about the static performance of the system. In particular, the plot allows determination of the error components as a function of X for any X_o, and in particular over the input range [X_o, $X_o+k\cdot\Delta X$] (in Fig. 10, as a reference, we highlighted the lines at $X = X_o$, $X_o+\Delta X$, and $X_o+4\cdot\Delta X$).

The relative deviation from linearity and the signal to noise ratio are the two criteria used to evaluate the static performance of the analogue optical link.

The total estimation error arising from both non-linearity and noise is:

$$\varepsilon_a(X,t) \equiv X_{est} - X = \varepsilon_{al}(X) - \frac{n(X,t)}{G}$$
$$\varepsilon_r(X,t) \equiv \frac{\varepsilon_a(X,t)}{X - X_0} = \varepsilon_{rl}(X) - \frac{n(X,t)}{G\cdot(X - X_0)} \qquad (8)$$

where the linearity errors $\varepsilon_{al}(X)$ and $\varepsilon_{rl}(X)$ have been defined in eq. 6.

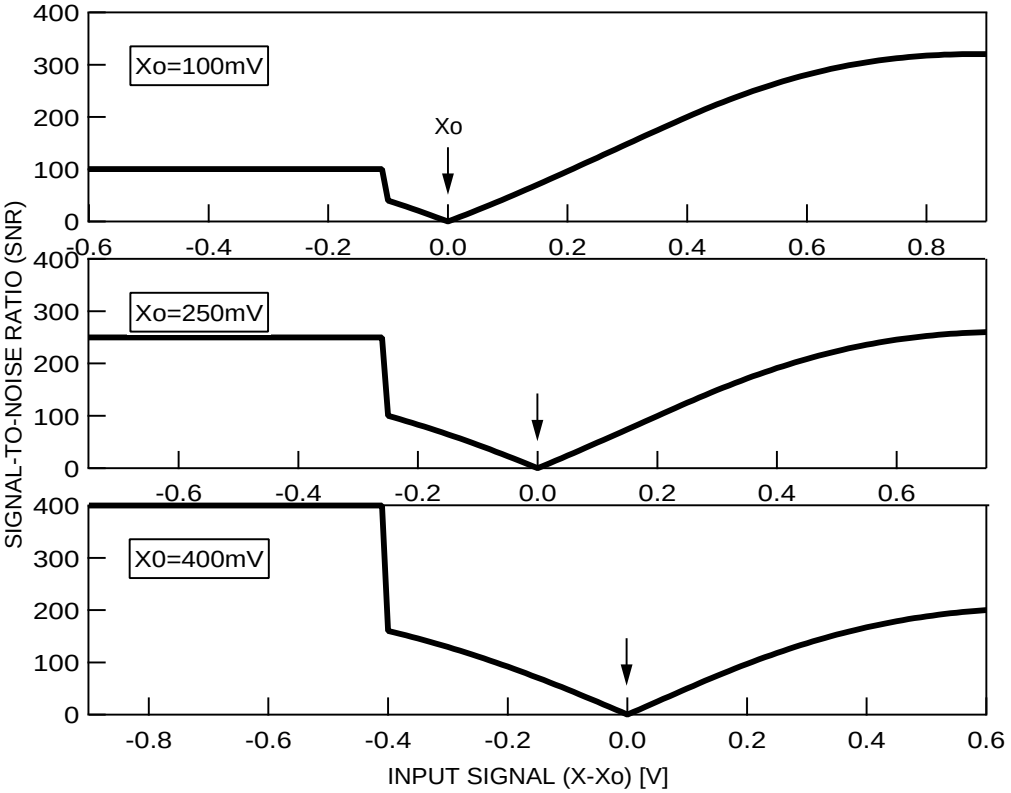

Figure 8: Signal-to-noise ratio as a function of X, for parameterised values of X_o. The system is the one modelled by the functions represented in Fig. 2.

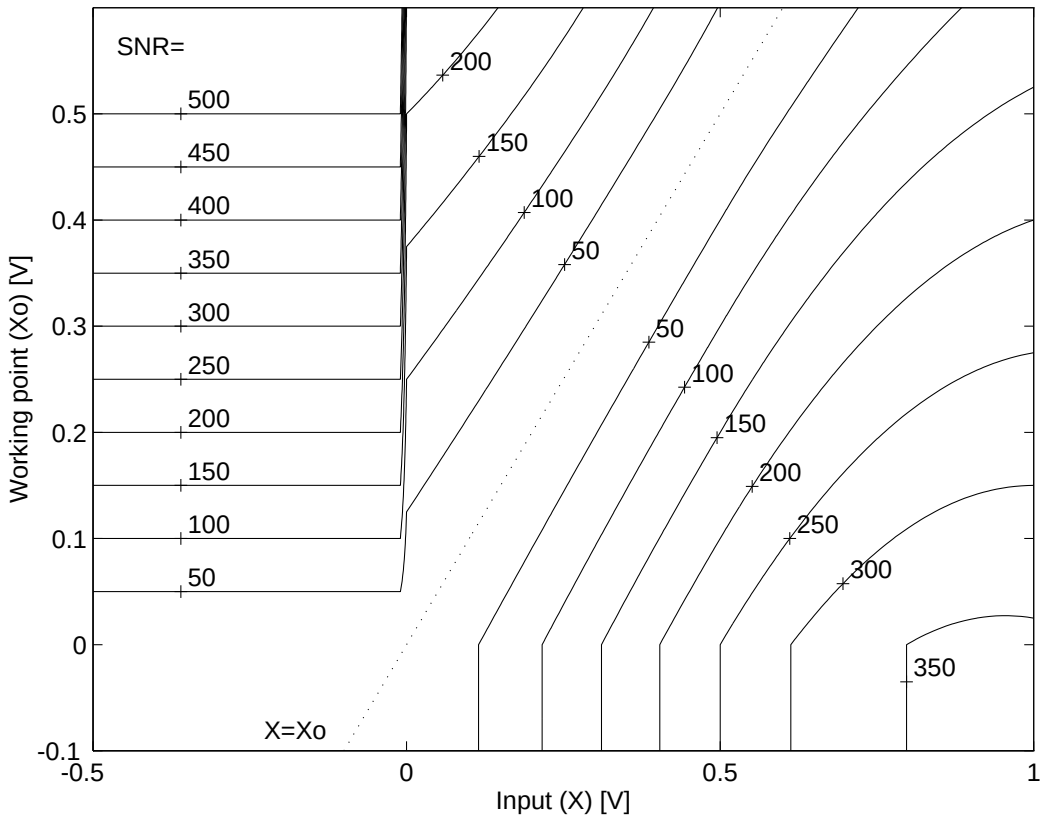

Figure 9: Contour plots representation of the signal-to-noise ratio in the (X, X_o) space. The system is the one modelled by the functions represented in Fig. 2.

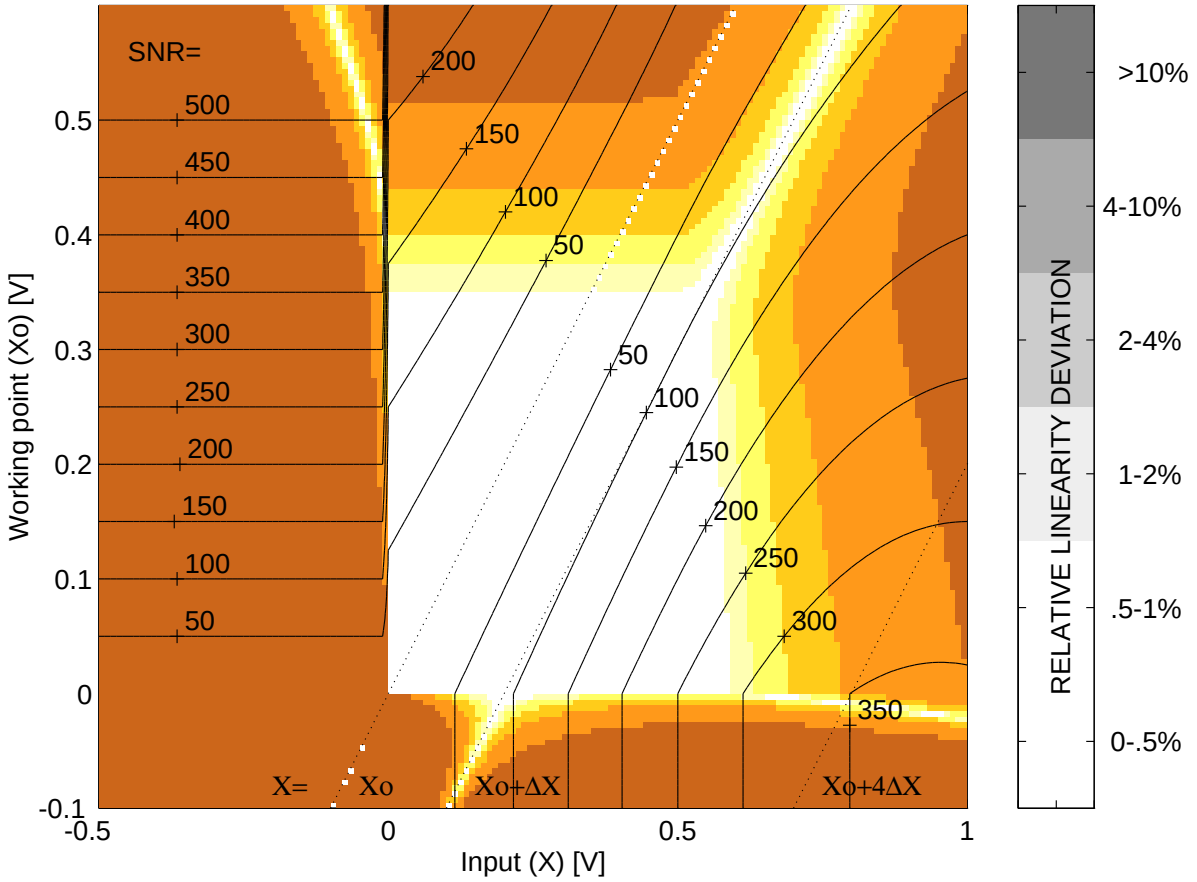

Figure 10: Compact representation of the static performance (linearity error and SNR) of the idealised system. The linearity error is represented with pseudo-colours, the SNR with contour plots. The system is the one modelled by the functions represented in Fig. 2.

In order to compare directly the magnitude of the linearity errors (systematic), the noise errors (stochastic), and the total errors (stochastic), the three are treated as if they were stochastic components, i.e. by considering their rms values.

The rms-value of the total estimation errors is the sum in quadrature of their mean (linearity errors) and standard deviation (rms-noise errors), which can be expressed in terms of the SNR as follows:

$$\begin{aligned}\left[\varepsilon_{\mathrm{a}}(X,t)_{RMS}\right]^2 &\equiv \overline{\varepsilon_{\mathrm{a}}^2(X,t)} = \varepsilon_{\mathrm{al}}^2(X) + \left(\frac{X - X_0 + \varepsilon_{\mathrm{al}}(X)}{\mathrm{SNR}(X)}\right)^2 \approx \varepsilon_{\mathrm{al}}^2(X) + \left(\frac{X - X_0}{\mathrm{SNR}(X)}\right)^2 \\ \left[\varepsilon_{\mathrm{r}}(X,t)_{RMS}\right]^2 &\equiv \overline{\varepsilon_{\mathrm{r}}^2(X,t)} = \varepsilon_{\mathrm{rl}}^2(X) + \left(\frac{1+\varepsilon_{\mathrm{rl}}(X)}{\mathrm{SNR}(X)}\right)^2 \approx \varepsilon_{\mathrm{rl}}^2(X) + \left(\frac{1}{\mathrm{SNR}(X)}\right)^2\end{aligned} \qquad (9)$$

where the approximated forms are valid only if $\varepsilon_{\mathrm{rl}}(X) << 1$.

Fig. 11 shows all the error components (absolute and relative) as a function of input signal: rms-noise errors are represented as dotted lines, linearity errors as dashed lines, and total rms-errors as solid lines. The appropriate balance between noise and linearity errors is found by adequately choosing the link operating range and calibration parameters.

Where the nonlinearity error dominates, this can be corrected for by use of linearisation techniques. Where the noise error dominates, signal processing can be applied to emphasise the signal against the noise or, if time is not critical, the noise can be filtered or averaged out.

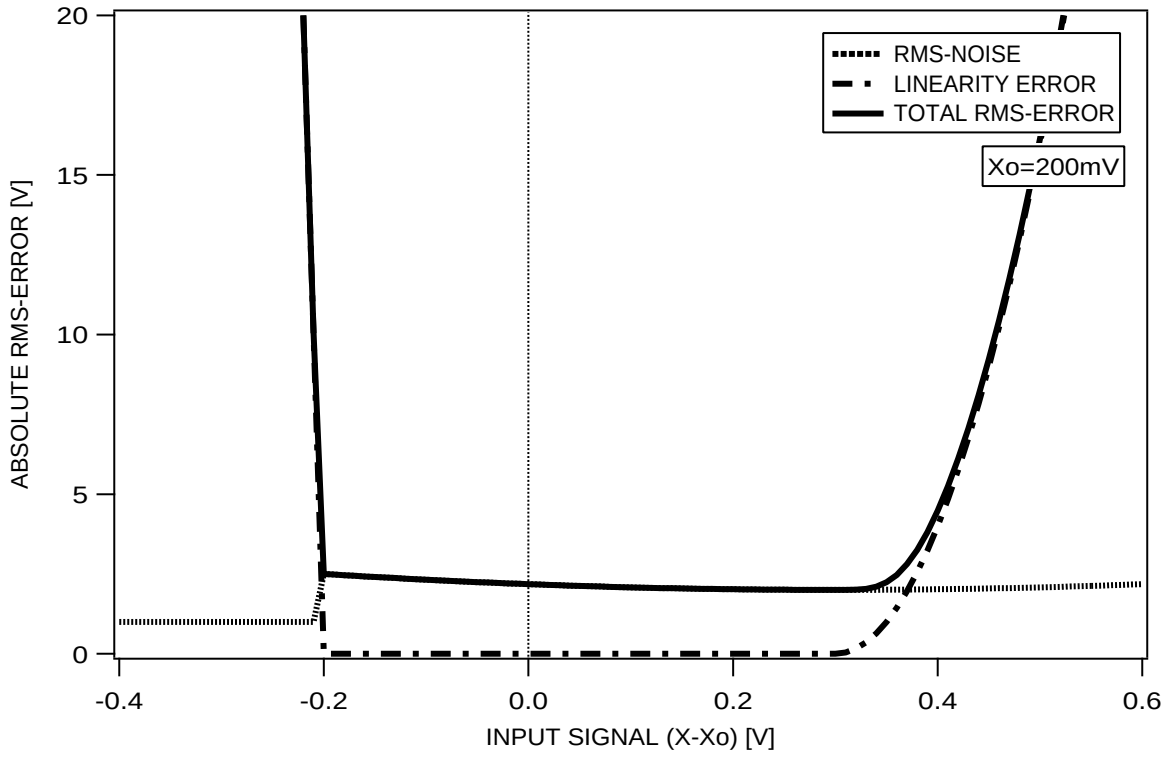

(a)

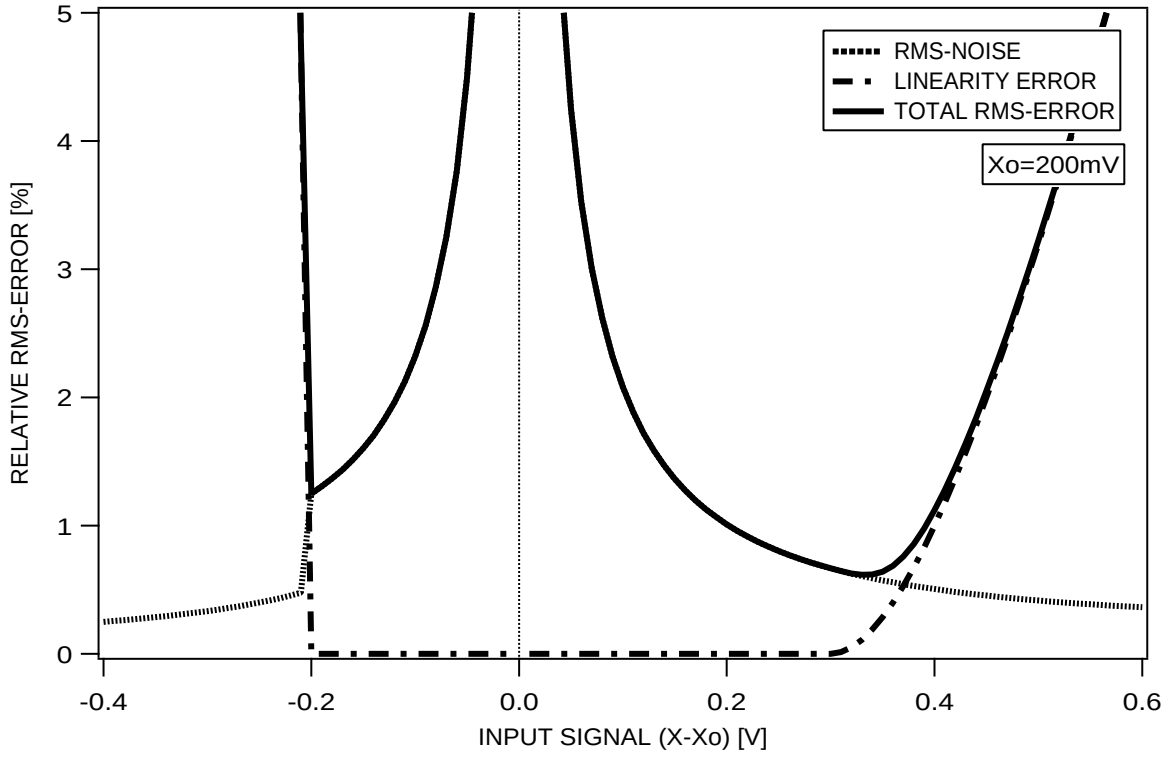

(b)

Figure 11: Total rms-errors as quadrature sum of the rms-noise error and of the linearity error: (a) absolute, and (b) relative representations.

5. Characterisation

The parameters X_o and ΔX should be adjusted so as to: (1) map the input range into the linear region; (2) maximise SNR; (3) leave enough margin to accommodate for the possible drifts of the transfer and noise characteristics; (4) minimise power dissipation. The optimisation procedure finds the best compromise between the criteria mentioned above.

Fig. 12 shows the results corresponding to the characterisation of a real optical link prototype, whose transfer and rms-noise functions are represented in Fig. 5, and for two choices of calibration pulse amplitude, ΔX=100 and 200 mV.

From the plots it is possible to see that a window with good linearity opens up in the working space. The corresponding ranges of X and X_o are limited at the bottom by the laser threshold (at X ~ -0.9 V) and at the top by the amplifier saturation (at X ~ 0.9 V). The working point X_o has to be chosen so that the whole input range fits into the 'linear' region of the transfer characteristic while maximising the achievable SNR.

The relative linearity error is better than 2% within most of the parameter space. The peak-SNR is quite constant as a function of X_o, but degrades for high values of X_o because of the higher noise in that region. Potentially the SNR can be as high as 1000:1. With some margin for threshold variations, a peak-SNR of 800:1 seems achievable.

From Fig. 12, it is apparent that the relative linearity error over the operating range is not critically dependent on the choice of the calibration pulse amplitude ΔX. A possible criterion to choose ΔX could be to define a region within the operating range where optimum linearity must be insured, and then to define the factor k>1 (see Section 2) for the top part of the range where linearity is not so critical. For the CMS Tracker application for instance, one might choose ΔX = 1 MIP and k = 4.

6. Tracking of the optical link performance

In the real environment we expect the characteristic optical link function $f(X)$ and the stochastic properties of the noise function $n(X,t)$ to be slowly varying with time. For instance, experimental results show that both the laser threshold and the laser efficiency vary, under exposure to radiation, temperature, and due to ageing [8]. Therefore, a re-calibration procedure for online tuning of the operational parameters X_o and G must be foreseen at regular intervals.

A small variation in the value of the parameter G can lead to a big degradation of the static performance of the system, whereas the choice of the parameter X_o affects the system common mode and is less critical, as long as the operating range is well within the linear region of the static transfer function (see Fig. 12). Based on these considerations, the re-calibration procedure of G should be relatively simple, so that it can be performed as often as possible, causing minimum dead time. On the other hand, the setting of X_o should be performed relatively seldom and only when necessary.

The definition of the parameter G given in eq. 4 is well adapted to a practical recalibration scheme where a pulse of known amplitude ΔX is generated by the front-end electronics. It allows accurate estimation of the system gain in the linear region, as shown by the evaluation results of a real optical link (see Fig. 12). A practical procedure for the setting of the working point X_o is still under discussion. This is only necessary when the laser threshold (time varying) is becoming too close to X_o (fixed at calibration time), and might be triggered by the laser output power going lower than a fixed minimum value.

7. Summary

A method for the static evaluation of analogue optical links in the laboratory has been developed. It relies on an automated setup for gain, rms-noise, and linearity measurements, and on a software program for off-line processing. Based on the measured data, the optical link static performance is evaluated as a function of the operational parameters X, X_o, ΔX. A compact representation of the results is described, where the two evaluation criteria (linearity error and signal-to-noise ratio) are visualised in the (X, X_o) working space. With the help of this representation, tuning of the operational parameters to optimise static performance of the system is straightforward, and the effect of various re-calibration schemes can be easily investigated.

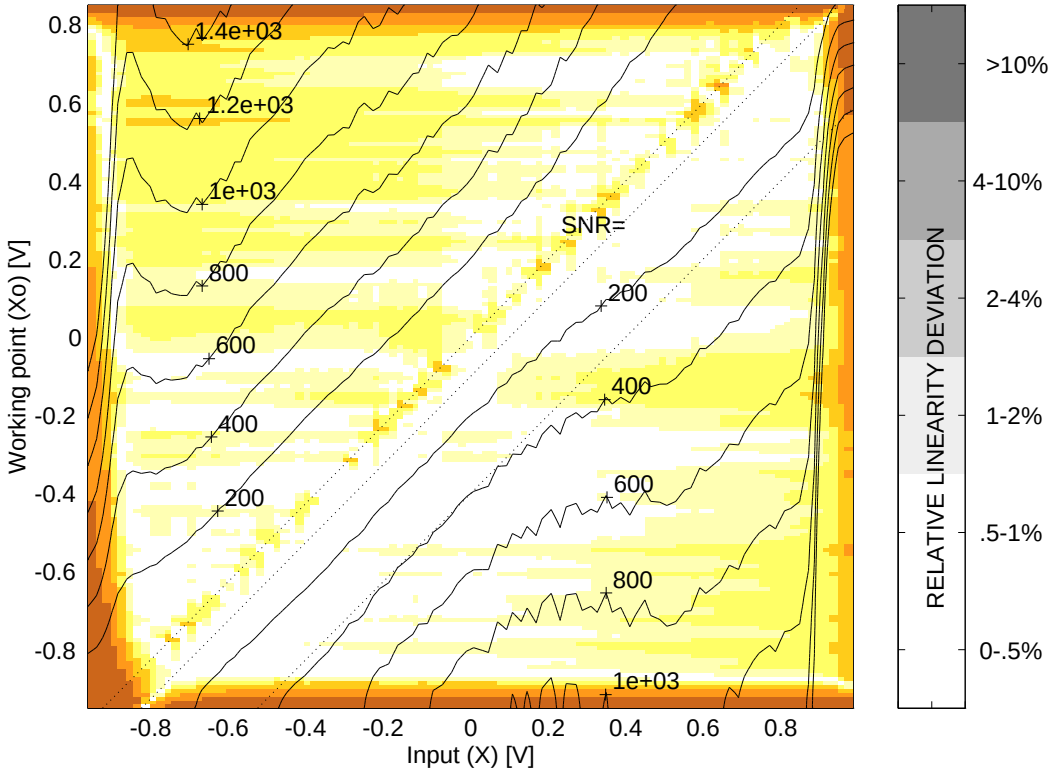

(a)

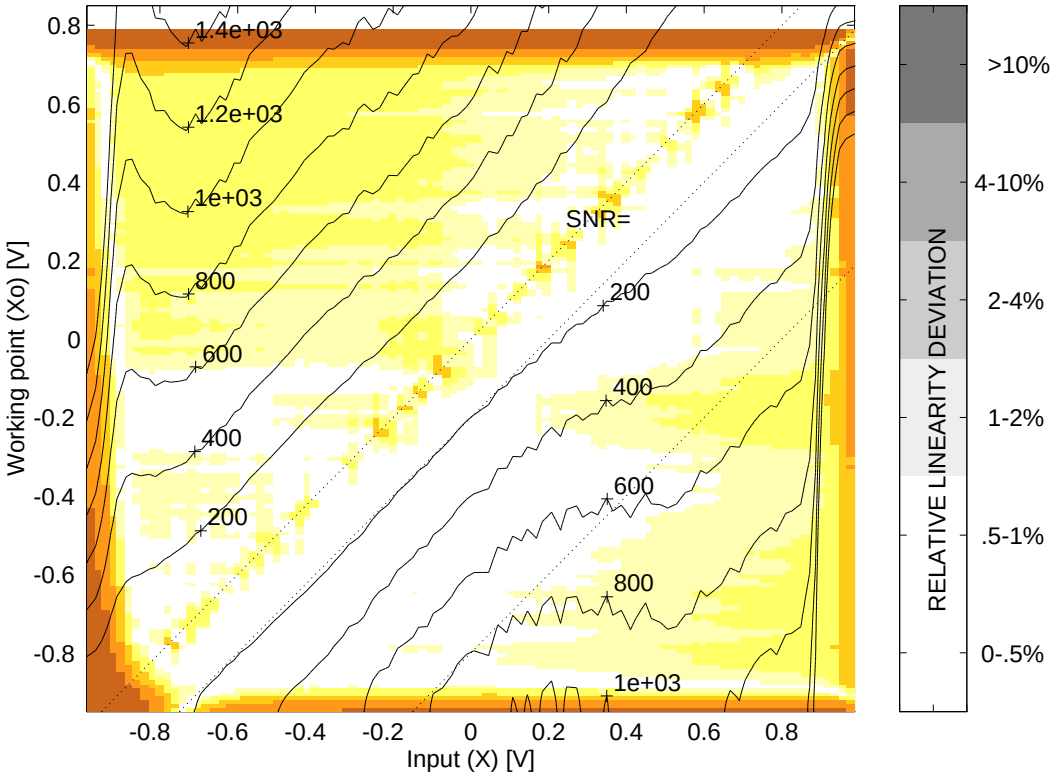

(b)

Figure 12: Static performance of the real optical link prototype for different amplitudes of the calibration pulse: (a) ΔX = 100 mV, and (b) ΔX = 200 mV.

As an example, a real optical link prototype has been successfully characterised. However, for the results to be generally relevant, a larger number of links must be measured, under different environmental conditions, and at different times. With an automated set-up and procedure, this can be done in a time effective manner. Systematic measurements are being carried out and results will be published in the near future.

Acknowledgements

This work is part of the doctoral thesis of G.Cervelli for the National Polytechnical Institute of Grenoble (INPG), coordinated by Prof. S.Tedjini (ENSERG/LEMO), and co-sponsored by ASSTP, Association for the Scientific and Technological Development of Piemonte, Italy. This work would have not been possible without the active collaboration of J.Wikiera (CERN Summer Student).

References

[1] CMS: The Tracker Project. Technical Design Report, CERN/LHCC 98-6, CMS TDR 5, April 1998.

[2] G.Hall, Analogue optical data transfer for the CMS tracker, Nuclear Instruments and Methods in Physics Research A 386 (1997) 138-142.

[3] F.Vasey, G.Stefanini, and G.Hall, Laser based optical links for the CMS tracker: options and choices, CMS Note 1997/053.

[4] F.Vasey et al., Development of rad-hard laser-based optical links for CMS front-ends, CERN/LHCC/97-60, Proceedings of the 3rd Workshop on Electronics for LHC Experiments, London, 1997.

[5] F.Vasey et al., Development of radiation-hard optical links for the CMS Tracker at CERN, IEEE Transaction on Nuclear Science, Vol. 45, No. 3, June 1998 (Proceedings of 1997 IEEE Nuclear Science Symposium, Albuquerque, New Mexico, November 1997).

[6] G.Cervelli et al., Time stability of an asymmetric Fabry-Perot modulator based analogue lightwave links, Journal of Lightwave Technology, Vol. 15, No. 8, 1997, pp. 1594-1601.

[7] V.Arbet-Engels et al., Analogue optical links for the CMS Tracker readout system, Nuclear Instruments And Methods In Physics Research A 409, 1998, pp. 634-638 (presented at the 7th Pisa Meeting on Advanced Detectors, Isola d'Elba, May 1997)

[8] K.Gill et al., Radiation damage studies of optoelectronic components for the CMS Tracker optical links, Proceeding of the 4th European Conference on Radiation and their Effects on Devices and Systems, RADECS, Cannes, 1997.